Gene expression and protein synthesis remodeling in response to iron deficiency in yeast

Hanna Barlit[1], Antonia María Romero[2], Ali Gülhan[1], Praveen K. Patnaik[1], Alexander Tyshkovskiy[3], María Teresa Martínez-Pastor[4], Vadim N. Gladyshev[3], Sergi Puig[2], Vyacheslav M. Labunskyy[1,*]

[1]Department of Dermatology, Boston University School of Medicine, Boston, United States

[2]Departamento de Biotecnología, Instituto de Agroquímica y Tecnología de Alimentos (IATA), Consejo Superior de Investigaciones Científicas (CSIC), Valencia, Spain

[3]Division of Genetics, Department of Medicine, Brigham and Women's Hospital, Harvard Medical School, Boston, United States

[4]Departamento de Bioquímica y Biología Molecular, Universitat de València, Valencia, Spain

[*]Correspondence: vlabuns@bu.edu

Abstract

Iron is an essential trace element that serves as a cofactor for enzymes involved in multiple metabolic pathways, including ribosome biogenesis, protein translation, DNA synthesis and repair, lipid metabolism, and mitochondrial oxidative phosphorylation. In eukaryotes, iron deficiency leads to coordinated changes in gene expression and protein translation that activate iron uptake and allow metabolic adaptations of iron-dependent processes. While transcriptional responses to iron deprivation have been extensively characterized, little is known about the role of iron in regulating protein synthesis. In this study, we performed a genome-wide analysis of protein translation in yeast to identify transcripts translationally regulated under iron deficiency. We show that, upon iron depletion, a large set of genes necessary for mitochondrial protein synthesis is specifically down-regulated at the translational level. We demonstrate that this regulation is mediated through the activity of Cth1 and Cth2 mRNA-binding proteins. In addition, we uncover that Fe deficiency affects protein translation by limiting the activity of the conserved ribosome recycling factor Rli1. Together, these studies identified genes and pathways that are translationally regulated in response to iron deficiency and revealed a role of iron in translational control.

Introduction

Iron (Fe) is an essential trace element that serves as a cofactor for enzymes involved in numerous cellular processes, including protein translation, DNA replication and repair, cholesterol and lipid biosynthesis, and mitochondrial oxidative phosphorylation (Zhang, 2014). Dysregulation of Fe homeostasis has been implicated in health and disease. In humans, Fe deficiency causes anemia and leads to the decline of immune, neuronal, and muscle functions (Andrews, 2000; Cronin et al., 2019). On the other hand, Fe overload leads to organ failure, due to Fe toxicity, and the development of several disorders, such as Alzheimer's disease, cancer, and delayed wound healing (Hare et al., 2013). Moreover, imbalance in Fe metabolism has been implicated in aging and age-associated organ failure, but the exact mechanisms remain unclear (Xu et al., 2012). A better understanding of the mechanisms by which cells adapt to changes in Fe availability is required for the development of targeted therapeutic strategies against diseases associated with the dysregulation of Fe homeostasis.

Yeast *Saccharomyces cerevisiae* has proven to be a useful model for understanding the basic mechanisms of adaptation of eukaryotic cells to Fe depletion. Previous studies have shown that Fe deficiency leads to significant changes in yeast gene expression (Puig et al., 2005; Romero et al., 2019; Shakoury-Elizeh et al., 2004). These changes are mediated by Aft1 and Aft2 transcription factors, which activate the transcription of ~35 genes known as the "Fe regulon". Expression of these genes allows cellular adaptation to low Fe through several mechanisms: (i) increasing Fe uptake into the cell, (ii) mobilizing Fe from vacuolar stores, and (iii) recycling iron by promoting heme degradation (Philpott and Protchenko, 2008; Ramos-Alonso et al., 2020; Shakoury-Elizeh et al., 2004). In addition, cells adapt to Fe deficiency by dropping the utilization of Fe for non-essential metabolic pathways and shifting to Fe-independent metabolism through the increased

expression of the mRNA binding protein Cth2, which is under the control of Aft1/2 transcription factors. Cth2 recognizes and binds to AU-rich sequences (5'-UAUUUAUU-3' and 5'-UUAUUUAU-3') in the 3'-untranslated region (UTR) of several mRNAs coding for proteins containing Fe as a cofactor (including aconitase, succinate dehydrogenase, and components of the mitochondrial electron transport chain) and stimulate their degradation (Puig et al., 2005). A paralog of Cth2, named Cth1, is 46% identical to Cth2, recognizes similar consensus sequences, and can repress the expression of a partially overlapping set of target genes (Puig et al., 2005; Puig et al., 2008; Ramos-Alonso et al., 2018). Thus, Cth1 and Cth2 remodel Fe metabolism prioritizing Fe for proteins involved in essential processes such as DNA replication and repair (Sanvisens et al., 2011).

Despite these studies thoroughly investigating changes in mRNA abundance in response to Fe deficiency, little is known about translational changes and how low Fe affects protein synthesis. Previous reports have shown that Fe deficiency leads to global inhibition of protein synthesis, which is dependent on TORC1 and Gcn2/eIF2α pathways (Romero et al., 2020; Romero *et al.*, 2019). In addition, Fe serves as a cofactor for several enzymes participating in protein translation, including proteins involved in modifications of factors affecting translation elongation, post-transcriptional transfer RNA (tRNA) modifications, translational termination, and ribosome recycling (Keeling et al., 2006; Romero et al., 2021; Young et al., 2015). Moreover, Cth2 has been shown to repress the translation of specific transcripts in response to Fe deficiency (Ramos-Alonso et al., 2018). However, changes in protein translation at the genome-wide level and the mechanisms of translational regulation by Fe have not been previously investigated. In this work, we applied RNA-Seq and ribosome profiling (Ribo-Seq) to yeast cells undergoing adaptation to Fe deficiency to quantitatively measure translational changes genome-wide. At the translation

level, we uncovered the down-regulation of a group of genes encoding components of the mitochondrial protein synthesis machinery in response to Fe depletion. We further show that this translational regulation is mediated by Cth1 and Cth2. We find that Fe deficiency also affects protein translation by dramatically decreasing the activity of the ribosome recycling factor Rli1. Importantly, eliminating Cth1 and Cth2 increased the levels of Rli1 indicating that cells adapt to Fe deficiency by limiting the activity of Rli1 in response to low Fe in a Cth1/2-dependent manner.

Results

Transcriptional and translational responses during the adaptation to iron deficiency.

Previous studies have shown that Fe deficiency in yeast *S. cerevisiae* leads to changes in transcriptional profiles (Hausmann et al., 2008; Puig et al., 2005; Shakoury-Elizeh et al., 2004). In addition, prolonged Fe deficiency has been shown to induce global inhibition of protein synthesis, which is dependent on the Gcn2/eIF2α pathway (Romero et al., 2020). However, little is known about how Fe deprivation manifests at the level of translational regulation. To distinguish the effects of Fe deficiency on mRNA abundance from its effects on protein translation, we performed RNA-Seq and ribosome profiling (Ribo-Seq) in wild-type W303a yeast cells cultured in Fe-sufficient (+Fe) or Fe-deficient conditions (-Fe), achieved by the addition of the Fe^{2+}-specific chelator bathophenanthroline disulfonate (BPS). For this, exponentially growing cells were isolated under Fe-sufficient conditions, and after a short- (3 h) or long-term (6 h) exposure to Fe deficiency (**Fig 1A, Dataset S1**). In addition to wild-type cells, we monitored genome-wide transcriptional and translational changes upon Fe limitation in the *cth1Δcth2Δ* mutant. The RNA-Seq and Ribo-Seq profiles showed significantly altered gene expression profiles during adaptation to low Fe from 0 h to 6 h of Fe deficiency, with intermediate changes at 3 h (**Fig S1**). Consistent

with previous studies, we also observed strong inhibition of global protein synthesis after 6 h of Fe deficiency in both wild-type cells and the *cth1Δcth2Δ* mutant as measured by polysome analysis, but changes at 3 h were less pronounced (**Fig 1B**). We found that most of the changes in translation (Ribo-Seq) during Fe deficiency correlated with the changes in mRNA abundance (RNA-Seq) (**Fig 1C**). These data demonstrate that the responses to Fe deficiency are mediated primarily by changes in mRNA levels. However, we also found a group of genes that were altered specifically at the translation level indicating that an additional level of regulation contributes to the response of yeast cells to Fe deficiency (**Fig 1D**).

Our analysis of the RNA-Seq and Ribo-Seq data revealed many of the previously known changes in response to Fe deficiency. Among the genes up-regulated during the time-course of Fe deficiency, we observed a number of Fe regulon genes that are controlled by the Aft1 and Aft2 transcription factors, including genes involved in Fe uptake, mobilization of Fe stores from the vacuole, and the metabolic changes to limit the use of Fe, which validated our experimental approach (Philpott et al., 2012; Ramos-Alonso et al., 2020). Genes up-regulated in response to Fe limitation were enriched in GO categories "iron ion homeostasis", "siderophore transport", "carbohydrate metabolic process", "glycolytic process", and "cellular amino acid catabolic process" (**Fig 1E**, **Dataset S2**). For example, expression of genes involved in Fe siderophore uptake (*FIT1-3, ARN1-4*), reductive Fe uptake (*FRE1-FRE4, FET3, FTR1, ATX1, CCC2, FET4*), and mobilization of vacuolar Fe (*FRE6, FET5, FTH1, SMF3*) increased several folds in response to Fe deprivation in wild-type cells (**Fig 1F** and **Fig S2**). We also observed that expression levels of *CTH2*, a gene coding for the mRNA-binding protein involved in metabolic remodeling in response to low Fe, were significantly induced in wild-type cells during Fe deficiency, whereas expression of its paralog *CTH1* was down-regulated at the level of transcript abundance.

Among the most enriched GO categories in genes down-regulated in response to Fe limitation were "cytoplasmic translation", "ribosomal large and small subunits", and "ribosome biogenesis" consistent with the overall inhibition of protein synthesis. However, there were substantial differences in down-regulated genes between wild-type and *cth1Δcth2Δ* cells. For example, "cellular respiration", "electron transport chain", "heme biosynthetic process", "iron-sulfur cluster assembly", "mitochondrial translation", and "tricarboxylic acid cycle" were enriched in down-regulated genes in wild-type cells, but not in the *cth1Δcth2Δ* mutant. In contrast, "rRNA processing" and "mitotic cell cycle" were specifically down-regulated in the *cth1Δcth2Δ* cells suggesting a role of Cth1 and Cth2 in regulation of these processes.

Ribo-Seq analyses demonstrate that mitochondrial ribosomal proteins are translationally regulated in response to Fe deficiency.

During Fe deficiency, yeast cells activate the expression of Cth2, an mRNA-binding protein involved in the remodeling of Fe metabolism. In response to low Fe, Cth2 post-transcriptionally inhibits the expression of several mRNAs that contain AU-rich elements (AREs) in the 3'-UTR (Puig et al., 2005; Ramos-Alonso et al., 2018). We expected that the lack of Cth1 and Cth2 in the *cth1Δcth2Δ* mutant would lead to the derepression of their targets. By comparing changes in protein synthesis profiles (Ribo-Seq) in wild-type and *cth1Δcth2Δ* cells we identified 164 genes that were translationally up-regulated in the *cth1Δcth2Δ* mutant compared to wild-type cells during 6 h of Fe deficiency (**Fig 2A** and **Dataset S1**). Among these translationally up-regulated genes, we found several previously reported targets of Cth1 and Cth2 that code for components of the electron transport chain (ETC) and tricarboxylic acid (TCA) cycle (**Fig 2B** and **Fig S3**) consistent with the known function of Cth1/2 mRNA-binding proteins in post-transcriptional regulation of

Fe-dependent genes (Puig et al., 2008; Ramos-Alonso et al., 2018). In addition to previously described Cth1/2 targets, these data uncovered that Cth1 and Cth2 are limiting the expression of genes encoding for mitochondrial ribosomal proteins (MRPs) (36 ribosomal proteins of the large subunit and 24 ribosomal proteins of the small subunit) as well as proteins involved in the assembly of the ETC (16 genes), mitochondrial translation (15 genes), protein translocation to mitochondria (10 genes), and ATP synthase assembly (4) (**Fig 2C**). However, very few of these Cth1/2-regulated genes contain AREs in their 3'UTRs within 500 nt after the stop codon (**Table 1**).

Amid the genes up-regulated during Fe deficiency in the *cth1Δcth2Δ* mutant, we identified *MYG1*. Myg1 is a 3'-5' RNA exonuclease that is involved in pre-ribosomal RNA processing and assembly of both cytoplasmic and mitochondrial ribosomes (Grover et al., 2019). Because this gene contains a putative ARE within its 3'UTR, we asked if this gene is directly regulated by Cth1/2 during Fe deficiency. Our data demonstrate that *MYG1* is down-regulated in response to low Fe in wild-type cells specifically at the mRNA level (but not in the *cth1Δcth2Δ* mutant), suggesting that *MYG1* is a direct Cth1/2 target (**Fig 2D**). In contrast, most of the genes encoding for MRP proteins lack ARE sequences in their 3'UTRs and Fe deficiency decreased their translation without affecting their transcript levels (**Fig 2D** and **Fig S4**). Notably, we found that mRNA transcripts encoding the Cbp3-Cbp4-Cbp6 complex, which is involved in the translation and assembly of the mitochondrial cytochrome bc1 complex, contain AREs in their 3'UTRs and are coordinately down-regulated by Cth1/2 in response to Fe deficiency (**Fig 2E**). Together, our results indicate that Cth1 and Cth2 directly and indirectly down-regulate multiple transcripts required for mitochondrial translation.

The effect of Fe deficiency on mitochondrial translation is mediated by Puf3 mRNA-binding protein.

To investigate how mitochondrial translation is regulated by Cth1/2, we monitored the expression of mitochondrial ribosomal proteins during the shift of cells from the fermentable carbon source to the non-fermentable medium containing glycerol that requires the induction of the mitochondrial ETC components and mitochondrial translation (Isaac et al., 2018). First, we analyzed publicly available Ribo-Seq data from cells undergoing a shift from the fermentable (Glu) to non-fermentable (Gly) media (Couvillion et al., 2016). As Fe is required for the synthesis of the ETC components, abrupt transfer from a fermentable to a non-fermentable carbon source results in transient activation of the Fe regulon genes including *CTH1* and *CTH2*, which are regulated by the Aft1 transcription factor (**Fig 3A** and **Fig S5A**). We also found that the synthesis of mitochondrial ribosomal proteins of the small subunit (MRPS) and large subunit (MRPL) was significantly decreased within 15 min of nutrient shift (**Fig 3A** and **Fig S5B**). However, prolonged incubation in glycerol-containing media resulted in a gradual increase in the synthesis of MRPs as mitochondrial translation is required for the adaptation to changes in carbon sources. The fact that expression of MRPs is negatively correlated with *CTH1* and *CTH2* and that genes encoding mitochondrial ribosomal proteins do not contain AREs suggests a possibility that these effects might be mediated by a Cth1/2 target that coordinately regulates them, but not directly.

Further analysis of genes translationally activated by Fe deficiency in the *cth1Δcth2Δ* mutant identified the presence of Puf3 binding sites in their 3'UTR sequences (**Table 1**). Puf3 is an RNA-binding protein that has been implicated in the control of mitochondrial translation (Gerber et al., 2004; Lapointe et al., 2015). In yeast, Puf3 senses glucose availability and binds to the 3'UTRs of mRNA transcripts involved in mitochondrial translation, including genes encoding components of

the mitochondrial large and small ribosomal protein subunits, promoting their degradation. However, upon glucose depletion, Puf3 becomes phosphorylated and switches its function to promote the translation of its target mRNAs (Lee and Tu, 2015). To test whether Cth1 and Cth2 regulate MRPs in a Puf3-dependent manner, we monitored phosphorylation of Puf3 during the time course of adaptation to the switch in carbon source in wild-type and *cth1Δcth2Δ* cells (**Fig 3B**). We observed that phosphorylation of Puf3 is increased during the switch to a non-fermentable carbon source in wild-type cells, consistent with prior studies. In contrast, Puf3 is constitutively phosphorylated in the *cth1Δcth2Δ* mutant even in the presence of high glucose. These data suggest that phosphorylated Puf3 could promote the translation of mitochondrial ribosome proteins in the *cth1Δcth2Δ* mutant when both fermentable and non-fermentable carbon sources are used. Together, these data support the possibility that Cth1 and Cth2 decrease the translation of mitochondrial ribosomal proteins and inhibit mitochondrial translation in wild-type cells in response to Fe deficiency through the increased activity of the Puf3 mRNA-binding protein.

Fe deficiency leads to increased ribosome occupancy in the 3'UTRs of genes due to decreased activity of Rli1.

Although overall protein synthesis is significantly reduced during Fe deficiency, how different steps of protein translation are affected by low Fe is not completely understood. Among enzymes participating in protein translation that require Fe as a cofactor, we selected Rli1 for further analysis. Rli1 is a conserved protein, which requires an iron-sulfur (Fe-S) cluster for its activity and is essential for translation termination and ribosome recycling (Romero et al., 2021). *RLI1* mRNA contains two putative AREs within its 3'UTR at 280 and 291 nt from its stop codon, and its transcript levels are upregulated in cells lacking *CTH1* and *CTH2* as compared to wild-type

cells in -Fe conditions (Puig et al., 2005; Puig et al., 2008) suggesting it is a direct Cth1/2 target mRNA. We expected that during Fe deficiency activity of Rli1 would decrease. Consistent with its function in ribosome recycling, we observed diminished Rli1 activity as evidenced by the accumulation of 80S ribosomes in the 3'UTRs of several mRNAs during prolonged Fe deficiency (6 h) in wild-type cells (**Fig. 4A** and **Fig S6**). In contrast, decrease in activity of the Rli1 was delayed in the *cth1Δcth2Δ* mutant. To investigate whether increased ribosome occupancy at 3'UTR in Fe depleted conditions is associated with active translation, we used yeast strains containing 3xHA tags in the 3'UTRs of *SED1* and *CWP2* (Young et al., 2015) downstream of the canonical stop codon (**Fig 4B**). We observed increased levels of 3'UTR translation products for *SED1* and *CWP2* during prolonged incubation of wild-type cells in the absence of Fe (**Fig 4B**). Western blot analysis revealed that these bands correspond to the production of small peptide products, rather than expected larger read-through events. Notably, eliminating Cth1 and Cth2 alleviated their repressive effects on the expression levels of *RLI1* during Fe deficiency in the *cth1Δcth2Δ* mutant (**Fig 4C**). Together, these data suggest that Fe deficiency decreases activity of Rli1 by promoting binding of Cth1/2 to the AREs in its 3'UTR and promoting degradation of its transcript.

Discussion

Although transcriptional responses to Fe deprivation have been extensively characterized, how Fe deficiency affects protein synthesis at the genome-wide level remained elusive. By combining RNA-Seq with the analysis of ribosome occupancy by Ribo-Seq, we quantitatively analyzed translatome changes in response to the short-term and prolonged Fe deficiency in yeast. This allowed us to identify groups of genes, whose expression was altered by low Fe specifically at

either transcriptional level or protein synthesis level, and provided mechanistic insights into the role of Fe in protein translation.

The changes in gene expression that we observed were consistent with prior studies that analyzed transcriptomic profiles during Fe deprivation showing altered expression of genes involved in Fe acquisition and mobilization (Puig et al., 2005; Shakoury-Elizeh et al., 2004). Expression of these genes is activated by the Aft1 and Aft2 transcription factors. In addition, we observed that Cth1 and Cth2 mRNA-binding proteins repress expression of their targets adjusting metabolism to prioritize Fe for essential processes (Philpott et al., 2012). For most of the transcripts, a strong correlation between RNA-Seq and Ribo-Seq profiles was found indicating that changes in gene expression induced by Fe deficiency predominantly occur at the level of transcription. However, we also identified a number of genes that were specifically down-regulated by Fe deficiency at the translation level (Fig. 2). These down-regulated proteins included components of the mitochondrial electron transport chain (ETC) and ETC assembly. In addition, mitochondrial ribosomal proteins and genes involved in mitochondrial translation were enriched among the genes that were translationally down-regulated, when Fe bioavailability was diminished. Inhibition of mitochondrial translation was not observed in previous reports because most of the prior studies focused solely on transcriptomic changes.

Importantly, we identified Cth1 and Cth2 as key factors that are responsible for the translational repression of mitochondrial ribosomes. Although the exact mechanisms of translational regulation by Cth1 and Cth2 remain unclear, we found that many of the genes translationally down-regulated by Fe deficiency contained binding sites for the Puf3 RNA-binding protein in their 3'UTRs. Puf3 is a known regulator of mitochondrial translation in response to glucose availability, which specifically binds to mRNA and represses translation of mitochondrial

ribosomal proteins (MRPs) (Gerber et al., 2004; Lapointe et al., 2018). In glucose-replete conditions, Puf3 degrades mRNA of MRPs limiting mitochondrial translation (Houshmandi and Olivas, 2005; Olivas and Parker, 2000), which aligns with known metabolism preferences of yeast for glucose utilization through fermentation. In contrast, glucose depletion or switch to non-fermentable carbon sources leads to Puf3 phosphorylation and the subsequent switch of its function from mRNA degradation to the facilitation of translation (Lee and Tu, 2015). Our data indicate that expression of Cth1 and Cth2 is inversely correlated with the levels of mitochondrial ribosomal proteins during the transition of yeast cells from high glucose media to media containing glycerol further supporting the role of Cth1 and Cth2 in regulation of mitochondrial translation. Nonfermentable carbon sources, such as glycerol, require expression of the components of the oxidative phosphorylation and active mitochondrial translation (Couvillion et al., 2016), suggesting that the activity of Cth1/2 and Puf3 may allow proper synchronization between mitochondrial translation and Fe levels and that this regulation is not only involved in acute response to Fe deficiency, but may also play a role in physiological, homeostatic processes. Supporting this idea, we recently found that increased expression of Cth2 is limiting the expression of mitochondrial ribosomal proteins during yeast replicative aging (Patnaik et al., 2022).

The fact that genes encoding MRPs lack AREs in their 3'UTR suggests that Cth1 and Cth2 may regulate translation of mitochondrial ribosomal proteins indirectly by affecting phosphorylation of the Puf3 mRNA-binding protein (Fig 3). However, the nature of the signal that leads to phosphorylation of Puf3 and specific kinases mediating the role of Cth1 and Cth2 in regulating mitochondrial translation warrants further investigation. Among potential candidates are PKA and Sch9, which have been shown to phosphorylate Puf3 when glucose becomes limited (Lee and Tu, 2015). In addition, phosphorylation of Puf3 in response to changes in the

mitochondrial membrane potential has been recently reported to promote mitochondrial biogenesis in several mutants lacking components of the mitochondrial ETC (Liu et al., 2021).

Another effect of Fe deficiency on translation was identified when 3'UTR sequences were analyzed. Ribosome profiling of Fe depleted cells revealed a striking decrease in the activity of the Fe-S cluster-containing Rli1 protein that serves as a ribosome recycling factor. We show that the number of footprints mapped to 3'UTR sequences was increased in Fe-deficient conditions to the same extent as seen previously in Rli1-depleted yeast cells (Young *et al.*, 2015) leading to generation of aberrant 3'UTR translation products (Fig 4). Notably, we observed delayed response in the *cth1Δcth2Δ* mutant indicating that Fe deficiency represses Rli1 function in wild-type cells as a result of Cth2-mediated post-transcriptional down-regulation of *RLI1* transcripts. These data suggest that yeast cells specifically down-regulate abundance of *RLI1* mRNA through Cth1 and Cth2 to limit Fe utilization by Rli1.

Together, our data demonstrate that Cth1 and Cth2 mRNA-binding proteins play an important role in regulation of protein synthesis in response to Fe deficiency by regulating activity of Puf3 protein, involved in the control of mitochondrial translation, and repressing ribosome recycling factor Rli1.

Materials and Methods

Yeast strains

The yeast strains used in this study and their genotypes are listed in Table S1. W303a and *cth1Δcth2Δ* cells were cultured at 30°C in liquid SD medium (0.17% yeast nitrogen base without ammonium sulfate and without amino acids, 2% D-glucose, and 2 g/L Kaiser drop-out (Formedium)). For induction of Fe deficiency, cells were initially grown to OD_{600} = 0.2 and Fe^{2+}

chelator bathophenanthrolinedisulfonic acid (BPS) was added to the final concentration 100 μM. Following the addition of BPS, cells were incubated for 3h and 6h. Cells were collected by rapid filtration through the 0.45 μm membrane filters using a glass holder filter assembly, scrapped with a spatula, and flash frozen in liquid nitrogen.

Library preparation for RNA-seq and ribosome profiling

Yeast extracts were prepared by cryogrinding the cell paste with BioSpec cryomill. The cell paste was re-suspended in lysis buffer (20mM Tris-HCl pH8, 140mM KCl, 5mM $MgCl_2$, 0.5mM DTT, 1% Triton X-100, 100 μg/mL cycloheximide), spun at 20,000xg at 4°C for 5 min and 1 mL of the supernatant was divided into two tubes, for total mRNAs and footprint extraction. For ribosome profiling 50 OD_{260} units of the lysate (in 1ml of lysis buffer) were treated with 10 μL units of RNase I (100 U/μL) for 1h with gentle rotation of samples at RT. Then, 1 ml of RNase-treated lysate was layered on a sucrose gradient for ultracentrifugation and monosome isolation. For RNA-seq samples poly(A) mRNA isolation was performed using a poly(A) mRNA isolation kit with subsequent mRNA fragmentation. All downstream steps of RNA-seq and ribosome profiling libraries preparation are common and were done as described previously (Beaupere et al., 2017) and sequenced using the Illumina HiSeq platform.

RNA-seq and Ribosome profiling data processing and analysis

During the pre-processing step of the data analysis, we used Cutadapt 4.1 package (Martin, 2011) to remove the adapter sequence and keep reads with a minimum length of 23 nucleotides. Next, we removed all reads mapped to rRNA sequences using an in-house script. Ribosomal footprint and total mRNA reads were aligned to the *S. cerevisiae* genome from the Saccharomyces Genome

Database (https://www.yeastgenome.org/, release number R64-2-1). Sequence alignment was performed using STAR software 2.7.1a, allowing two mismatches per read (Dobin et al., 2013). Counts were generated with featureCounts from Rsubread 1.22.2 package (Liao et al., 2019).

Differential expression analysis

Counts generated in the previous step were saved as an expression matrix and used for differential expression analysis. For this purpose, first, we filtered out genes with less than 10 counts in less than 66.6% of samples (an empirically chosen threshold aiming to bring the distribution of the counts closer to normal and preserve the maximum number of genes with minimal variation between replicates). After filtering step, we obtained 5506 genes in RNA-Seq and 5069 genes in Ribo-Seq expression matrices. To identify differentially expressed genes, we used the generalized linear model of the EdgeR package (GLM, glmFit, glmLRT). In particular, we performed pairwise comparisons between samples subjected to Fe-deficiency (for 3h and 6h) and control samples – '3H/0H' and '6H/0H' comparisons, Moreover, we compared expression patterns between W303a and *cth1Δcth2Δ* mutant within timepoints to identify *CTH2*-dependent processes. We considered genes as differentially expressed if adjusted P-values (FDR) < 0.05 (Robinson et al., 2010). Differentially expressed genes are presented in Dataset S1.

Ribosome occupancy analysis

To estimate translational efficiency changes in old cells, we analyzed ribosomal occupancy (RO), which represents a ratio between ribosomal footprints and mRNA abundance and, thus, allows us to identify actively translated transcripts. To calculate RO, first, genes with low counts (less than 10 counts) were filtered out from RNA-Seq and Ribo-Seq datasets containing raw counts. RNA-

Seq and Ribo-Seq data were next RLE normalized ("Relative Log Expression" normalization) using the edgeR package (Robinson et al., 2010). Finally, we calculated RO using the formula: log2 (Ribo-seq counts +1) – log2 (RNA-seq counts + 1). Limma R package was used to estimate the statistical significance of RO data. Considering the nature of RO data, we considered genes to be differentially expressed when P-values adjusted (FDR) < 0.1 (Anders and Huber, 2010; Ritchie et al., 2015).

RT-qPCR

Total RNA was isolated by hot acid phenol extraction. RNA was treated with DNaseI, and 1 µg of RNA was used for cDNA synthesis using SuperScript III reverse transcriptase (Thermo Fisher Scientific) with random hexamer primers according to manufacturer's instructions. mRNA expression was then analyzed by real-time PCR using KAPA SYBR FAST qPCR Master Mix (Kapa Biosystems) and the CFX-96 Touch Real-Time PCR Detection System (Bio-Rad Laboratories). *ACT1* was used as a reference gene for normalization of mRNA expression between genotypes. Results are represented as means ± SEM from three independent experiments.

Western blot analysis

Yeast total extracts were prepared using TCA precipitation. 5OD of cells were resuspended in 0.5 mL of 6% TCA , incubated at least 10 min on ice and centrifuged for 5 min at 4°C at maximum speed (~14000 x g). Then, the pellet was washed twice with acetone and air-dried. Once dry, the pellet was resuspended in 250 µL of HU buffer (5 M urea, 50 mM Tris-HCl pH 7.5, 1% SDS, 1 mM PMSF) and glass beads were added, and samples were homogenized by vortexing at

maximum speed for 10 x 30 sec. After that, samples were centrifuged, supernatant was transferred to fresh 1.5 mL tubes and concentration of lysates was normalized using Pierce BCA Protein Assay Kit. After normalization, sample buffer and BME (final concentration of 5%) were added. We used 4% hand-made gels for Puf3 phosphorylation status analysis and 12% Bis-Tris NuPAGE gels for translation re-initiation analysis. Anti-HA-Peroxidase, High Affinity (3F10) rat monoclonal antibody (Roche) was used to detect HA-tagged proteins. Mouse anti-Pgk1 monoclonal antibody (Life Technologies) was used as a primary antibody and Mouse IgGκ light chain binding protein (m-IgGκBP) conjugated to horseradish peroxidase (Santa Cruz Biotechnology) was used as a secondary antibody to detect Pgk1.

Quantification and statistical analysis

Statistical analysis was performed using Prism 9.3.1 (GraphPad Software, Inc). Statistical significance of the RT-qPCR data was determined by calculating p values using one-way ANOVA. Error bars represent standard errors of the means (SEM). The information about number of replicates and P values can be found in figure legends. For RNA-Seq and Ribo-Seq analyses tree biological replicates were analyzed per each condition.

Data availability

Raw reads and processed sequencing data generated by this study have been deposited in the GEO database (www.ncbi.nlm.nih.gov/geo/; Accession: GSE193025)

Acknowledgments

We would like to thank Dr. Alan Hinnebusch for providing yeast strains containing 3xHA tags in the 3'UTRs of *SED1* and *CWP2* used in this study. This work was supported by NIH Grants AG058713 and AG066704 to VML, and grant PID2020-116940RB-I00 from MCIN/AEI/10.13039/501100011033 to SP.

Competing interests

The authors declare no competing interests.

References

Anders, S., and Huber, W. (2010). Differential expression analysis for sequence count data. Genome Biol *11*, R106. 10.1186/gb-2010-11-10-r106.

Andrews, N.C. (2000). Iron Metabolism: Iron Deficiency and Iron Overload. Annual Review of Genomics and Human Genetics *1*, 75-98. 10.1146/annurev.genom.1.1.75.

Beaupere, C., Chen, R.B., Pelosi, W., and Labunskyy, V.M. (2017). Genome-wide quantification of translation in budding yeast by ribosome profiling. J Vis Exp *130*, e56820. 10.3791/56820.

Couvillion, M.T., Soto, I.C., Shipkovenska, G., and Churchman, L.S. (2016). Synchronized mitochondrial and cytosolic translation programs. Nature *533*, 499-503. 10.1038/nature18015.

Cronin, S.J.F., Woolf, C.J., Weiss, G., and Penninger, J.M. (2019). The Role of Iron Regulation in Immunometabolism and Immune-Related Disease. Frontiers in Molecular Biosciences *6*. 10.3389/fmolb.2019.00116.

Dobin, A., Davis, C.A., Schlesinger, F., Drenkow, J., Zaleski, C., Jha, S., Batut, P., Chaisson, M., and Gingeras, T.R. (2013). STAR: ultrafast universal RNA-seq aligner. Bioinformatics *29*, 15-21. 10.1093/bioinformatics/bts635.

Gerber, A.P., Herschlag, D., and Brown, P.O. (2004). Extensive association of functionally and cytotopically related mRNAs with Puf family RNA-binding proteins in yeast. PLoS Biol *2*, E79. 10.1371/journal.pbio.0020079.

Grover, R., Burse, S.A., Shankrit, S., Aggarwal, A., Kirty, K., Narta, K., Srivastav, R., Ray, A.K., Malik, G., Vats, A., et al. (2019). Myg1 exonuclease couples the nuclear and mitochondrial translational programs through RNA processing. Nucleic Acids Res *47*, 5852-5866. 10.1093/nar/gkz371.

Hare, D., Ayton, S., Bush, A., and Lei, P. (2013). A delicate balance: Iron metabolism and diseases of the brain. Frontiers in Aging Neuroscience *5*. 10.3389/fnagi.2013.00034.

Hausmann, A., Samans, B., Lill, R., and Muhlenhoff, U. (2008). Cellular and mitochondrial remodeling upon defects in iron-sulfur protein biogenesis. J Biol Chem *283*, 8318-8330. 10.1074/jbc.M705570200.

Houshmandi, S.S., and Olivas, W.M. (2005). Yeast Puf3 mutants reveal the complexity of Puf-RNA binding and identify a loop required for regulation of mRNA decay. RNA *11*, 1655-1666. 10.1261/rna.2168505.

Isaac, R.S., McShane, E., and Churchman, L.S. (2018). The Multiple Levels of Mitonuclear Coregulation. Annu Rev Genet *52*, 511-533. 10.1146/annurev-genet-120417-031709.

Keeling, K.M., Salas-Marco, J., Osherovich, L.Z., and Bedwell, D.M. (2006). Tpa1p is part of an mRNP complex that influences translation termination, mRNA deadenylation, and mRNA turnover in Saccharomyces cerevisiae. Mol Cell Biol *26*, 5237-5248. 10.1128/MCB.02448-05.

Lapointe, C.P., Stefely, J.A., Jochem, A., Hutchins, P.D., Wilson, G.M., Kwiecien, N.W., Coon, J.J., Wickens, M., and Pagliarini, D.J. (2018). Multi-omics Reveal Specific Targets of the RNA-Binding Protein Puf3p and Its Orchestration of Mitochondrial Biogenesis. Cell Syst *6*, 125-135 e126. 10.1016/j.cels.2017.11.012.

Lapointe, C.P., Wilinski, D., Saunders, H.A., and Wickens, M. (2015). Protein-RNA networks revealed through covalent RNA marks. Nat Methods *12*, 1163-1170. 10.1038/nmeth.3651.

Lee, C.D., and Tu, B.P. (2015). Glucose-Regulated Phosphorylation of the PUF Protein Puf3 Regulates the Translational Fate of Its Bound mRNAs and Association with RNA Granules. Cell Rep *11*, 1638-1650. 10.1016/j.celrep.2015.05.014.

Liao, Y., Smyth, G.K., and Shi, W. (2019). The R package Rsubread is easier, faster, cheaper and better for alignment and quantification of RNA sequencing reads. Nucleic Acids Res *47*, e47. 10.1093/nar/gkz114.

Liu, S., Liu, S., He, B., Li, L., Li, L., Wang, J., Cai, T., Chen, S., and Jiang, H. (2021). OXPHOS deficiency activates global adaptation pathways to maintain mitochondrial membrane potential. EMBO Rep *22*, e51606. 10.15252/embr.202051606.

Martin, M. (2011). Cutadapt removes adapter sequences from high-throughput sequencing reads. 2011 *17*, 3. 10.14806/ej.17.1.200.

Olivas, W., and Parker, R. (2000). The Puf3 protein is a transcript-specific regulator of mRNA degradation in yeast. EMBO J *19*, 6602-6611. 10.1093/emboj/19.23.6602.

Patnaik, P.K., Beaupere, C., Barlit, H., Romero, A.M., Tsuchiya, M., Muir, M., Martinez-Pastor, M.T., Puig, S., Kaeberlein, M., and Labunskyy, V.M. (2022). Deficiency of the RNA-binding protein Cth2 extends yeast replicative lifespan by alleviating its repressive effects on mitochondrial function. Cell Rep *40*, 111113. 10.1016/j.celrep.2022.111113.

Philpott, C.C., Leidgens, S., and Frey, A.G. (2012). Metabolic remodeling in iron-deficient fungi. Biochim Biophys Acta *1823*, 1509-1520. 10.1016/j.bbamcr.2012.01.012.

Philpott, C.C., and Protchenko, O. (2008). Response to iron deprivation in Saccharomyces cerevisiae. Eukaryot Cell *7*, 20-27. 10.1128/EC.00354-07.

Puig, S., Askeland, E., and Thiele, D.J. (2005). Coordinated remodeling of cellular metabolism during iron deficiency through targeted mRNA degradation. Cell *120*, 99-110. 10.1016/j.cell.2004.11.032.

Puig, S., Vergara, S.V., and Thiele, D.J. (2008). Cooperation of two mRNA-binding proteins drives metabolic adaptation to iron deficiency. Cell Metab *7*, 555-564. 10.1016/j.cmet.2008.04.010.

Ramos-Alonso, L., Romero, A.M., Martinez-Pastor, M.T., and Puig, S. (2020). Iron Regulatory Mechanisms in Saccharomyces cerevisiae. Front Microbiol *11*, 582830. 10.3389/fmicb.2020.582830.

Ramos-Alonso, L., Romero, A.M., Soler, M.A., Perea-Garcia, A., Alepuz, P., Puig, S., and Martinez-Pastor, M.T. (2018). Yeast Cth2 protein represses the translation of ARE-containing mRNAs in response to iron deficiency. PLoS Genet *14*, e1007476. 10.1371/journal.pgen.1007476.

Ritchie, M.E., Phipson, B., Wu, D., Hu, Y., Law, C.W., Shi, W., and Smyth, G.K. (2015). limma powers differential expression analyses for RNA-sequencing and microarray studies. Nucleic Acids Res *43*, e47. 10.1093/nar/gkv007.

Robinson, M.D., McCarthy, D.J., and Smyth, G.K. (2010). edgeR: a Bioconductor package for differential expression analysis of digital gene expression data. Bioinformatics *26*, 139-140. 10.1093/bioinformatics/btp616.

Romero, A.M., Martinez-Pastor, M.T., and Puig, S. (2021). Iron in Translation: From the Beginning to the End. Microorganisms *9*. 10.3390/microorganisms9051058.

Romero, A.M., Ramos-Alonso, L., Alepuz, P., Puig, S., and Martinez-Pastor, M.T. (2020). Global translational repression induced by iron deficiency in yeast depends on the Gcn2/eIF2alpha pathway. Sci Rep *10*, 233. 10.1038/s41598-019-57132-0.

Romero, A.M., Ramos-Alonso, L., Montella-Manuel, S., Garcia-Martinez, J., de la Torre-Ruiz, M.A., Perez-Ortin, J.E., Martinez-Pastor, M.T., and Puig, S. (2019). A genome-wide

transcriptional study reveals that iron deficiency inhibits the yeast TORC1 pathway. Biochim Biophys Acta Gene Regul Mech *1862*, 194414. 10.1016/j.bbagrm.2019.194414.

Sanvisens, N., Bano, M.C., Huang, M., and Puig, S. (2011). Regulation of ribonucleotide reductase in response to iron deficiency. Mol Cell *44*, 759-769. 10.1016/j.molcel.2011.09.021.

Shakoury-Elizeh, M., Tiedeman, J., Rashford, J., Ferea, T., Demeter, J., Garcia, E., Rolfes, R., Brown, P.O., Botstein, D., and Philpott, C.C. (2004). Transcriptional remodeling in response to iron deprivation in Saccharomyces cerevisiae. Mol Biol Cell *15*, 1233-1243. 10.1091/mbc.e03-09-0642.

Xu, J., Jia, Z., Knutson, M.D., and Leeuwenburgh, C. (2012). Impaired Iron Status in Aging Research. International Journal of Molecular Sciences *13*, 2368-2386.

Young, D.J., Guydosh, N.R., Zhang, F., Hinnebusch, A.G., and Green, R. (2015). Rli1/ABCE1 Recycles Terminating Ribosomes and Controls Translation Reinitiation in 3'UTRs In Vivo. Cell *162*, 872-884. 10.1016/j.cell.2015.07.041.

Zhang, C. (2014). Essential functions of iron-requiring proteins in DNA replication, repair and cell cycle control. Protein & Cell *5*, 750-760. 10.1007/s13238-014-0083-7.

Figure Legends

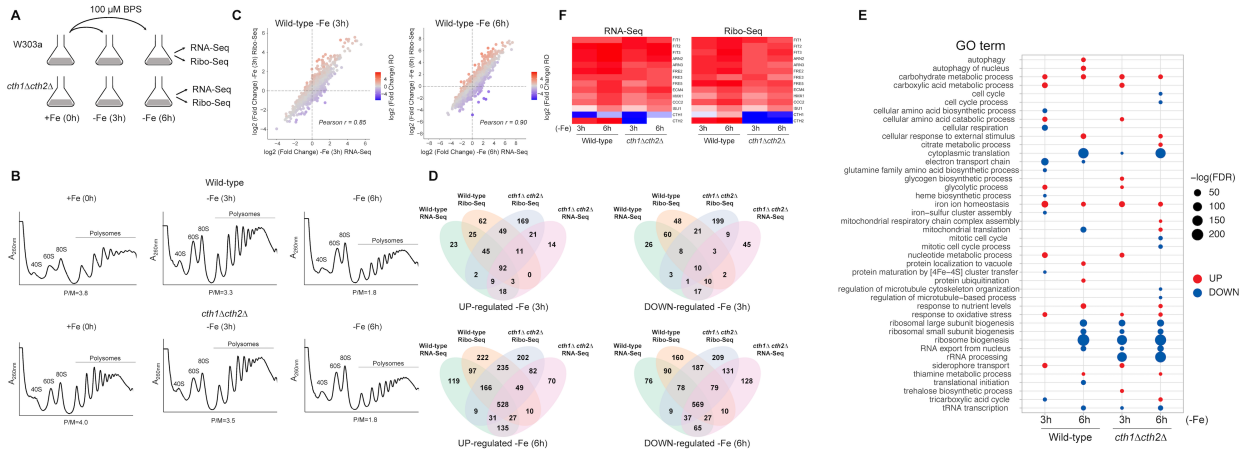

Fig. 1. Coordinated changes in mRNA levels and translation allow metabolic reprogramming in response to low Fe. A) Experimental design. **B**) Polysome profiles of wild-type and *cth1Δcth2Δ* cells during the time-course of Fe deficiency. Polysome to monosome (P/M) ratios were calculated using areas under the curve using ImageJ. Corresponding monosome (40S, 60S, 80S) and polysome peaks are indicated. **C**) Comparison of transcriptional (RNA-Seq) and translational (Ribo-Seq) changes during the course of Fe deficiency. Genes whose ribosome occupancy (RO) is increased (red) or decreased (blue) during Fe deficiency are highlighted. **D**) Venn diagrams show genes whose transcription (RNA-Seq) and translation (Ribo-Seq) were significantly changed during Fe deficiency (FDR<0.05). **E**) GO terms enriched among translationally up- and down-regulated genes during Fe deficiency. **F**) RNA-Seq and Ribo-Seq expression profiles of Fe regulon genes. Heatmaps show log2 fold change in mRNA abundance (RNA-Seq) and protein translation (Ribo-Seq) compared to untreated (0 h) samples.

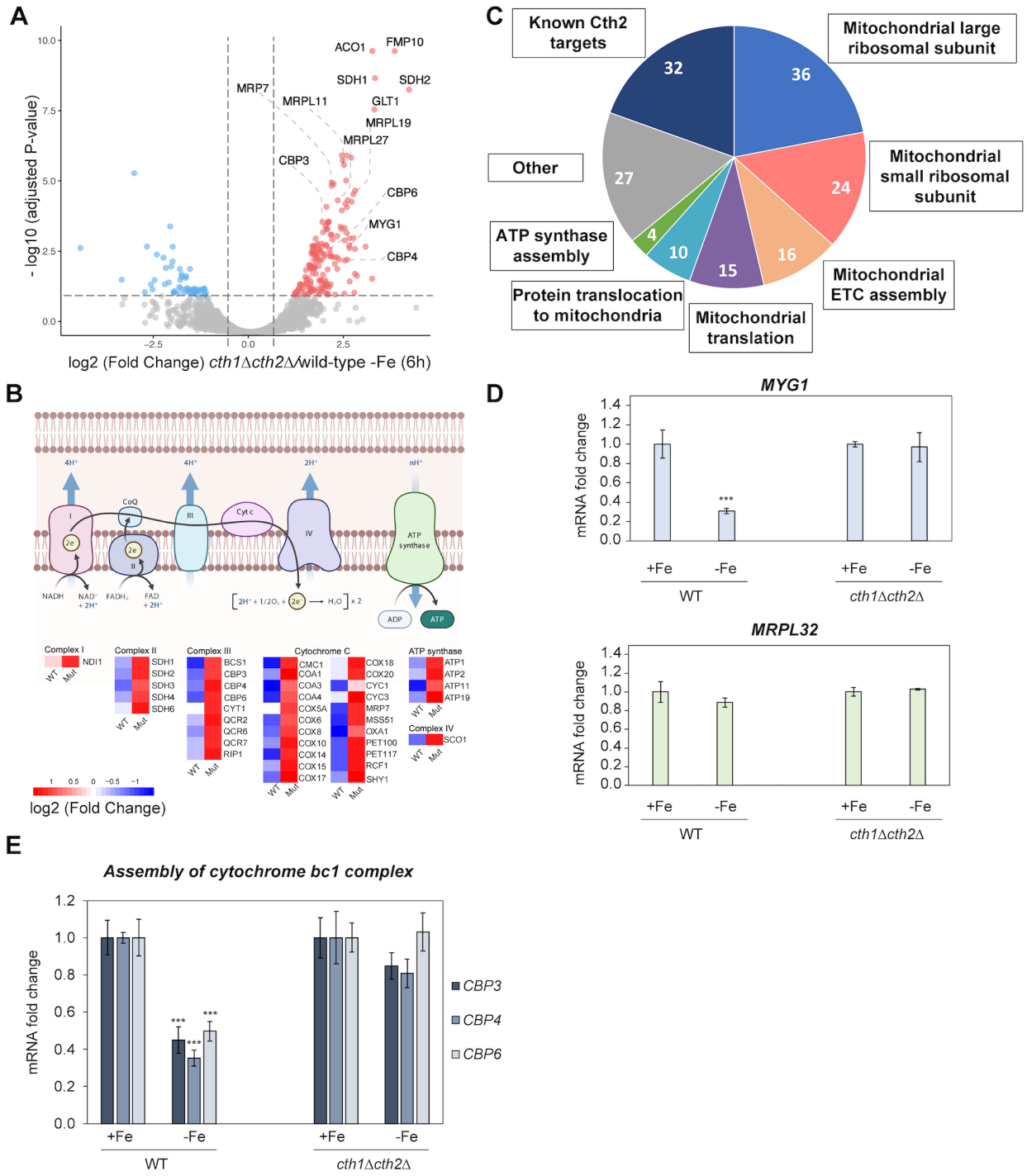

Fig 2. Fe deficiency leads to Cth1/2-dependent inhibition of mitochondrial translation. A) Volcano plot of differentially regulated genes in the *cth1Δcth2Δ* mutant compared to wild-type cells at 6 h (-Fe). **B**) Heatmap of differentially regulated genes of ETC in *cth1Δcth2Δ* compared to wild-type cells (FDR<0.05). **C**) Pie chart of genes activated in the *cth1Δcth2Δ* compared to wild-type cells. **D)** Translation of mitochondrial ribosomal proteins is regulated by Fe deficiency in a Cth1/2-dependent manner without affecting mRNA transcript levels. The expression of *MYG1* and

MRPL32 was determined by RT-qPCR. Error bars represent SEM of three independent experiments, ***$p<0.001$ (one-way ANOVA). **D)** Fe deficiency coordinately downregulates expression of transcripts encoding the Cbp3-Cbp4-Cbp6 complex. The expression of *CBP3, CBP4,* and *CBP6* was determined by RT-qPCR. Error bars represent SEM of three independent experiments, ***$p<0.001$ (one-way ANOVA).

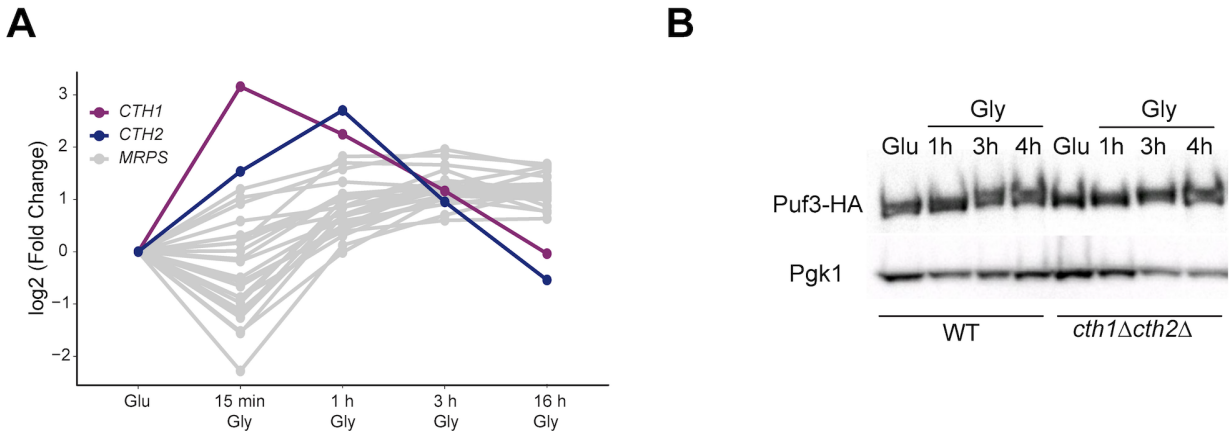

Fig 3. The effect of Fe deficiency on the expression of mitochondrial ribosomal proteins is mediated by Puf3 mRNA-binding protein. A) Expression of mitochondrial ribosomal proteins of the small subunit (*MRPS*) during the shift from the fermentable to non-fermentable carbon source is negatively correlated with the expression of *CTH1* and *CTH2*. Cells were grown in YPD (Glu) or YPG (Gly) for the indicated time. Fold change in protein translation was measured by Ribo-Seq. **B**) Wild-type and *cth1Δcth2Δ* cells expressing *PUF3*-HA were incubated in glucose medium (Glu) to log phase and shifted to glycerol (Gly) medium for the indicated time. Puf3 expression was assessed by western blot analysis.

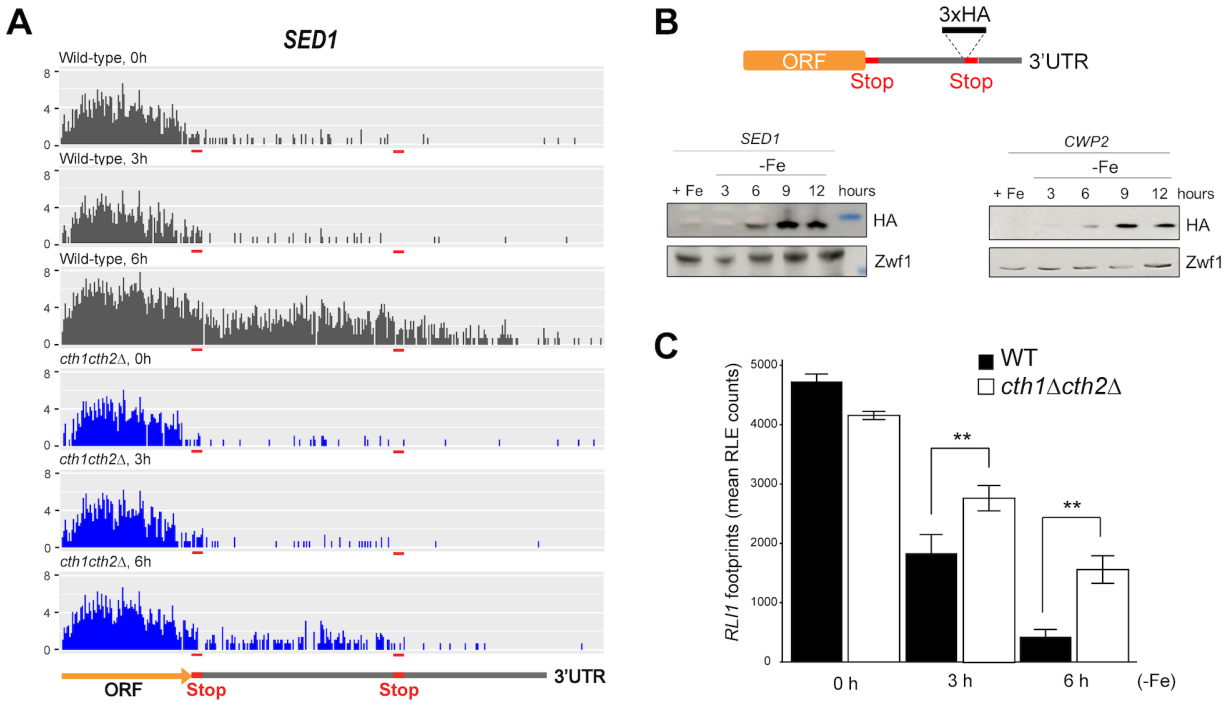

Fig 4. Fe deficiency leads to increased translation of 3'UTRs due to Cth1/2-dependent inhibition of Rli1 activity. A) Ribosome occupancy at the 3'UTR of *SED1* mRNA during short (3h) and prolonged (6h) Fe deficiency (-Fe). The location of the translation termination site is shown with red boxes. **B**) Strains containing 3xHA tags inserted in the 3'UTRs of *SED1* and *CWP2* (Young et al., 2015) show increased translation downstream of the canonical translation stop codon during prolonged Fe deficiency. Strains expressing tagged proteins were cultured in Fe sufficient (+Fe) media and after Fe deficiency (-Fe) for the indicated time. The expression of tagged proteins was detected by western blot analysis with HA-tag antibodies. **C**) Lack of Cth1/2 in the *cth1Δcth2Δ* mutant leads to derepression of *RLI1*. Error bars represent SEM of three independent experiments, **p<0.01 (one-way ANOVA).

Table 1. Location of putative AU-rich elements (AREs) and Puf3 binding sites in genes translationally regulated by yeast Cth1/Cth2 proteins in response to Fe deficiency.

Gene	Function	Putative AREs	Puf3 sites
Known Cth2 targets (32)			
ACO1	Aconitase required for the tricarboxylic acid (TCA) cycle	32,150,177	
APE4	Cytoplasmic aspartyl aminopeptidase	33	
CCC1	Vacuolar Fe^{2+}/Mn^{2+} transporter	24,144	
CCP1	Mitochondrial cytochrome-c peroxidase	18,41,50,59	
CIR2	Mitochondrial protein with similarity to flavoprotein dehydrogenase	13,37,81	
CLU1	Subunit of the eukaryotic translation initiation factor 3 (eIF3)	23	58
COX10	Heme A:farnesyltransferase		50
DPH2	Protein required for synthesis of diphthamide of translation elongation factor 2		359
FMP10	Protein of unknown function found in mitochondria	15,23	51
GLT1	NAD(+)-dependent glutamate synthase (GOGAT)	15,37,45,53,61,69,77	
HAP4	Heme activator protein	275, 304	
HEM1	5-aminolevulinate synthase	103,140	
HEM15	Ferrochelatase, catalyzes the insertion of ferrous iron into protoporphyrin IX	44,100	
ISA1	Protein required for maturation of mitochondrial [4Fe-4S] proteins	46,62	
ILV3	Dihydroxyacid dehydratase involved in biosynthesis of branched-chain amino acids	98	
KGD1	Subunit of the mitochondrial alpha-ketoglutarate dehydrogenase complex	193,230	
LEU1	Isopropylmalate isomerase involved in the leucine biosynthesis pathway	85,123	
LIP5	Protein involved in biosynthesis of the coenzyme lipoic acid	70,92,124	178
NFU1	Protein involved in Fe-S cluster transfer to mitochondrial clients	192,204	52

QCR2	Subunit 2 of the ubiquinol cytochrome-c reductase complex	155	
QCR6	Subunit 6 of the ubiquinol cytochrome-c reductase complex	31	
QCR8	Subunit 8 of the ubiquinol cytochrome-c reductase complex	97,114	
RIP1	Ubiquinol-cytochrome-c reductase	293,355	
RLI1	Essential Fe-S protein required for ribosome biogenesis and translation initiation	280,291	
RNR4	Ribonucleotide-diphosphate reductase (RNR) small subunit	39,125	
SDH1	Flavoprotein subunit of succinate dehydrogenase	153,164,180,188,196,204	97
SDH2	Iron-sulfur protein subunit of succinate dehydrogenase	163,309,328	196
SDH3	Subunit of succinate dehydrogenase	90	
SDH4	Membrane anchor subunit of succinate dehydrogenase	122,136,159	
TRP1	Phosphoribosylanthranilate isomerase	16	315
WTM1	Transcriptional repressor involved in regulation of meiosis, silencing, and expression of RNR genes	145	
YNL320W	Putative protein of unknown function	92	

Mitochondrial ribosomal protein (large subunit) (36)

IMG1	Mitochondrial ribosomal protein of the large subunit		31
IMG2	Mitochondrial ribosomal protein of the large subunit		30
MHR1	Mitochondrial ribosomal protein of the large subunit		56
MNP1	Mitochondrial ribosomal protein of the large subunit		77,154
MRP7	Mitochondrial ribosomal protein of the large subunit		50
MRPL1	Mitochondrial ribosomal protein of the large subunit		26,85
MRPL3	Mitochondrial ribosomal protein of the large subunit		16,51

MRPL4	Mitochondrial ribosomal protein of the large subunit		26
MRPL6	Mitochondrial ribosomal protein of the large subunit		84
MRPL7	Mitochondrial ribosomal protein of the large subunit		80,210,236
MRPL8	Mitochondrial ribosomal protein of the large subunit		25
MRPL9	Mitochondrial ribosomal protein of the large subunit		31
MRPL10	Mitochondrial ribosomal protein of the large subunit		52
MRPL11	Mitochondrial ribosomal protein of the large subunit		52
MRPL13	Mitochondrial ribosomal protein of the large subunit		45
MRPL15	Mitochondrial ribosomal protein of the large subunit		59
MRPL17	Mitochondrial ribosomal protein of the large subunit		87
MRPL19	Mitochondrial ribosomal protein of the large subunit		85,23
MRPL20	Mitochondrial ribosomal protein of the large subunit		25
MRPL22	Mitochondrial ribosomal protein of the large subunit	259	134
MRPL25	Mitochondrial ribosomal protein of the large subunit		76
MRPL27	Mitochondrial ribosomal protein of the large subunit	2	28
MRPL31	Mitochondrial ribosomal protein of the large subunit		41
MRPL32	Mitochondrial ribosomal protein of the large subunit	75	44,69
MRPL33	Mitochondrial ribosomal protein of the large subunit		56,163
MRPL35	Mitochondrial ribosomal protein of the large subunit		27
MRPL36	Mitochondrial ribosomal protein of the large subunit		100,136,422
MRPL37	Mitochondrial ribosomal protein of the large subunit		31
MRPL40	Mitochondrial ribosomal protein of the large subunit	254	106
MRPL44	Mitochondrial ribosomal protein of the large subunit		86

MRPL49	Mitochondrial ribosomal protein of the large subunit	11,39
MRPL50	Mitochondrial ribosomal protein of the large subunit	35
MRPL51	Mitochondrial ribosomal protein of the large subunit	46
RML2	Mitochondrial ribosomal protein of the large subunit	119
RTC6	Mitochondrial ribosomal protein of the large subunit	64,96
YML6	Mitochondrial ribosomal protein of the large subunit	7,79

Mitochondrial ribosomal protein (small subunit) (24)

EHD3	Mitochondrial ribosomal protein of the small subunit	54,88
MRP1	Mitochondrial ribosomal protein of the small subunit	49,81
MRP2	Mitochondrial ribosomal protein of the small subunit	48
MRP4	Mitochondrial ribosomal protein of the small subunit	35
MRP13	Mitochondrial ribosomal protein of the small subunit	39
MRP17	Mitochondrial ribosomal protein of the small subunit	39,199
MRP21	Mitochondrial ribosomal protein of the small subunit	52,89
MRP51	Mitochondrial ribosomal protein of the small subunit	28,44
MRPS5	Mitochondrial ribosomal protein of the small subunit	6,68
MRPS8	Mitochondrial ribosomal protein of the small subunit	58
MRPS9	Mitochondrial ribosomal protein of the small subunit	137,330
MRPS12	Mitochondrial ribosomal protein of the small subunit	72
MRPS18	Mitochondrial ribosomal protein of the small subunit	61
MRPS28	Mitochondrial ribosomal protein of the small subunit	27
MRPS35	Mitochondrial ribosomal protein of the small subunit	26,68
NAM9	Mitochondrial ribosomal protein of the small subunit	53

PET123	Mitochondrial ribosomal protein of the small subunit		109
RSM7	Mitochondrial ribosomal protein of the small subunit		20
RSM19	Mitochondrial ribosomal protein of the small subunit	293	8,36
RSM24	Mitochondrial ribosomal protein of the small subunit		31
RSM25	Mitochondrial ribosomal protein of the small subunit		37
RSM26	Mitochondrial ribosomal protein of the small subunit		35,86
RSM27	Mitochondrial ribosomal protein of the small subunit		49,147
RSM28	Mitochondrial ribosomal protein of the small subunit		30
Mitochondrial electron transport chain assembly (16)			
BCS1	Protein required for complex III assembly		27
CBP3	Mitochondrial protein required for assembly of cytochrome bc1 complex III	38	134
CBP4	Mitochondrial protein required for assembly of cytochrome bc1 complex III	80, 248	94
CBP6	Mitochondrial protein required for assembly of cytochrome bc1 complex III	33	21
CMC2	Protein involved in respiratory chain complex assembly		50
COA1	Mitochondrial protein required for assembly of the cytochrome c oxidase complex (complex IV)		22
COA4	win Cx(9)C protein involved in cytochrome c oxidase organization		25
COX14	Mitochondrial cytochrome c oxidase (complex IV) assembly factor		140
COX17	Metallochaperone required for copper delivery to cytochrome c oxidase (complex IV)		30,75
CYT2	Cytochrome c1 heme lyase involved in maturation of cytochrome c1		16

HSP60	Tetradecameric mitochondrial chaperonin		57
MSS51	Specific translational activator for the mitochondrial *COX1* mRNA		92
PET100	Chaperone that facilitates the assembly of cytochrome c oxidase (complex IV)	55	70
PET117	Assembly factor that couples heme a synthesis to complex IV assembly		46
SCO1	Copper-binding protein required for cytochrome c oxidase (complex IV)		27,66
TCM62	Protein involved in assembly of the succinate dehydrogenase (complex II)		40
Mitochondrial translation (15)			
AIM10	Mitochondrial protein with similarity to tRNA synthetases		31
IFM1	Mitochondrial translation initiation factor 2		102,125
MEF1	Mitochondrial translation elongation factor		25,123
MSD1	Mitochondrial aspartyl-tRNA synthetase		63,92
MSE1	Mitochondrial glutamyl-tRNA synthetase		37
MSK1	Mitochondrial lysine-tRNA synthetase		24,46
MST1	Mitochondrial threonyl-tRNA synthetase		24,106
MSY1	Mitochondrial tyrosyl-tRNA synthetase		24,76
MSC6	Multicopy suppressor of HER2 involved in mitochondrial translation		81
MTO1	Mitochondrial protein involved in mitochondrial tRNA modification		25
MYG1	3′-5′ RNA exonuclease involved in regulation of mitochondrial translation	59	
NAM2	Mitochondrial leucyl-tRNA synthetase		31,117
RPM2	Protein subunit of mitochondrial RNase P	19	

RRF1	Mitochondrial ribosome recycling factor		40
TUF1	Mitochondrial translation elongation factor Tu		87,188
Protein translocation to mitochondria (10)			
MBA1	Membrane-associated mitoribosome receptor		6,37,350
MIA40	Component of MIA pathway		54
MSP1	AAA-ATPase involved in mitochondrial protein sorting		101
PAM16	Subunit of the import motor component of the translocase TIM23 complex		110
PAM18	Subunit of the import motor component of the translocase TIM23 complex		126,141
SSC1	Hsp70 family ATPase import motor component of the TIM23 complex		
TAM41	Mitochondrial phosphatidate cytidylyltransferase	110	
TIM17	Essential component of the translocase TIM23 complex	309	2,158
TOM20	Component of the TOM complex		47,189
XDJ1	Chaperone involved in mitochondrial protein import		54
ATP synthase assembly (4)			
ATP11	Molecular chaperone required for the assembly of the mitochondrial F1/F0 ATP synthase		54
ATP12	Assembly factor for the mitochondrial F1/F0 ATP synthase		71
ATP2	Beta subunit of the mitochondrial F1/F0 ATP synthase		230
FMC1	Mitochondrial protein required for assembly of the mitochondrial F1/F0 ATP synthase		28,55
Other (27)			
ADH6	NADPH-dependent medium chain alcohol dehydrogenase		135
AIM32	2Fe-2S mitochondrial protein involved in redox quality control	87	

AIM36	Protein of unknown function		53
COQ1	Hexaprenyl pyrophosphate synthetase involved in ubiquinone biosynthesis		79
COQ6	Flavin-dependent monooxygenase involved in ubiquinone biosynthesis	42	5
DPC29	Putative mitochondrial protein of unknown function		40
FLX1	Mitochondrial flavin adenine dinucleotide transporter		31
HEM3	Porphobilinogen deaminase	102,251	263
IBA57	Protein involved in incorporating iron-sulfur clusters into proteins		16
LIP2	Lipoyl ligase		126
MAM33	Protein involved in mitochondrial ribosome assembly		62
MAS2	Alpha subunit of the mitochondrial processing protease		213
MGP12	Mitochondrial glutaredoxin-like protein		29
MIX23	Mitochondrial intermembrane space protein of unknown function		48
MRX15	Membrane-associated mitoribosome receptor		24,61
MRX20	Putative mitochondrial transport protein		26
NAT2	N-terminal acetyltransferase		23
POA1	Phosphatase that is highly specific for ADP-ribose 1"-phosphate	42	
PHB1	Subunit of the prohibitin complex		64
PHB2	Subunit of the prohibitin complex		109
PUF3	mRNA-binding protein involved in regulation of nuclear-encoded mitochondrial proteins		369
RIM2	Mitochondrial pyrimidine nucleotide transporter	164	
RKM5	Protein lysine methyltransferase involved in modification of the ribosomal large subunit Rpl1a/Rpl1b		286

RMD9	Mitochondrial protein that controls mitochondrial gene expression		40,99
YFH1	Mitochondrial matrix iron chaperone	26	
YLF2	Protein of unknown function		17
YML002W	Putative protein of unknown function		

AREs, AU-rich elements (5'-UUAUUUAU-3' and 5'-UAUUUAUU-3' octamers) located within 500 nucleotides downstream of the translation termination stop codon.

Puf3 sites, predicted 10 nt Puf3 (C/U)(A/C/U)UGUA(A/U)AUA binding elements located within 500 nucleotides downstream of the translation termination stop codon.

Supplementary Figures

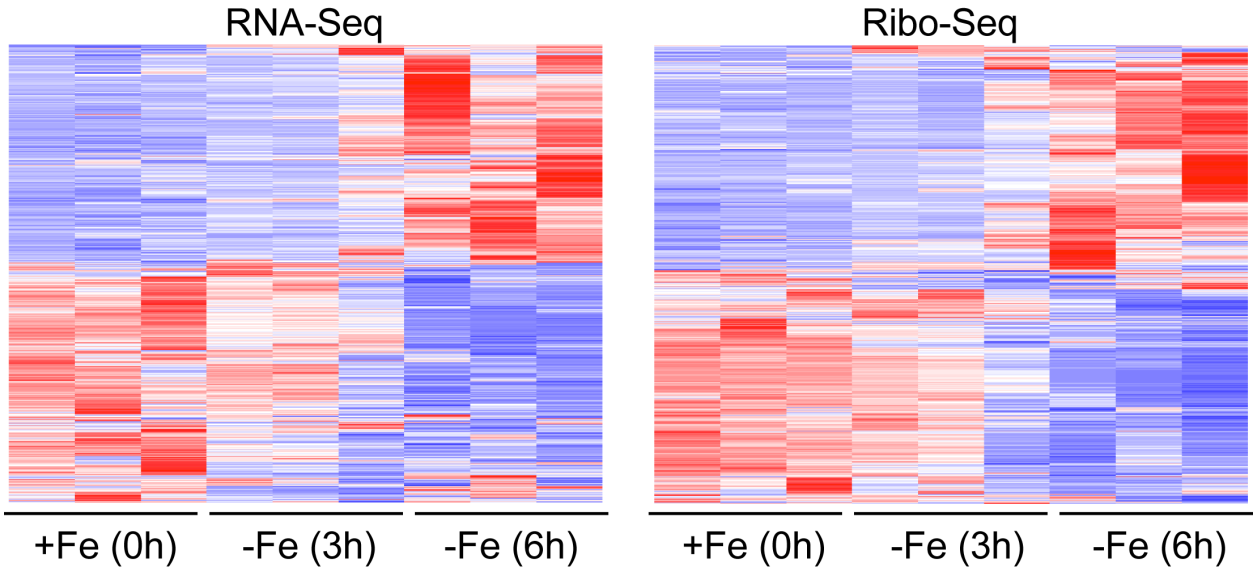

Fig. S1. Changes in RNA-Seq and Ribo-Seq expression profiles in response to Fe deficiency. Heatmaps show changes in transcription (RNA-Seq) and protein translation (Ribo-Seq) scaled expression values (RLE-normalized log2 read counts) in wild-type cells during short-term (3h) and prolonged (6h) Fe deficiency.

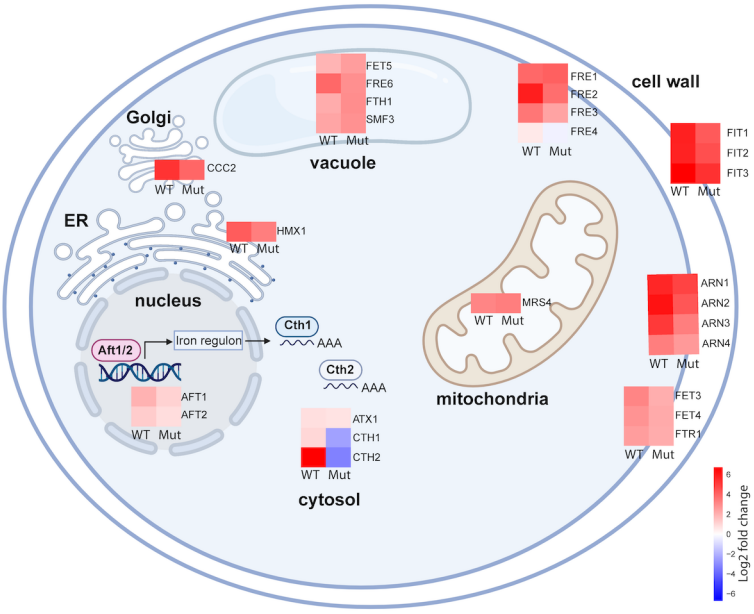

Fig. S2. Heatmaps show log2 fold change in protein translation (Ribo-Seq) of Fe regulon genes during prolonged (6h) Fe deficiency in wild-type (WT) cells and the *cth1Δcth2Δ* mutant (Mut) (FDR<0.05).

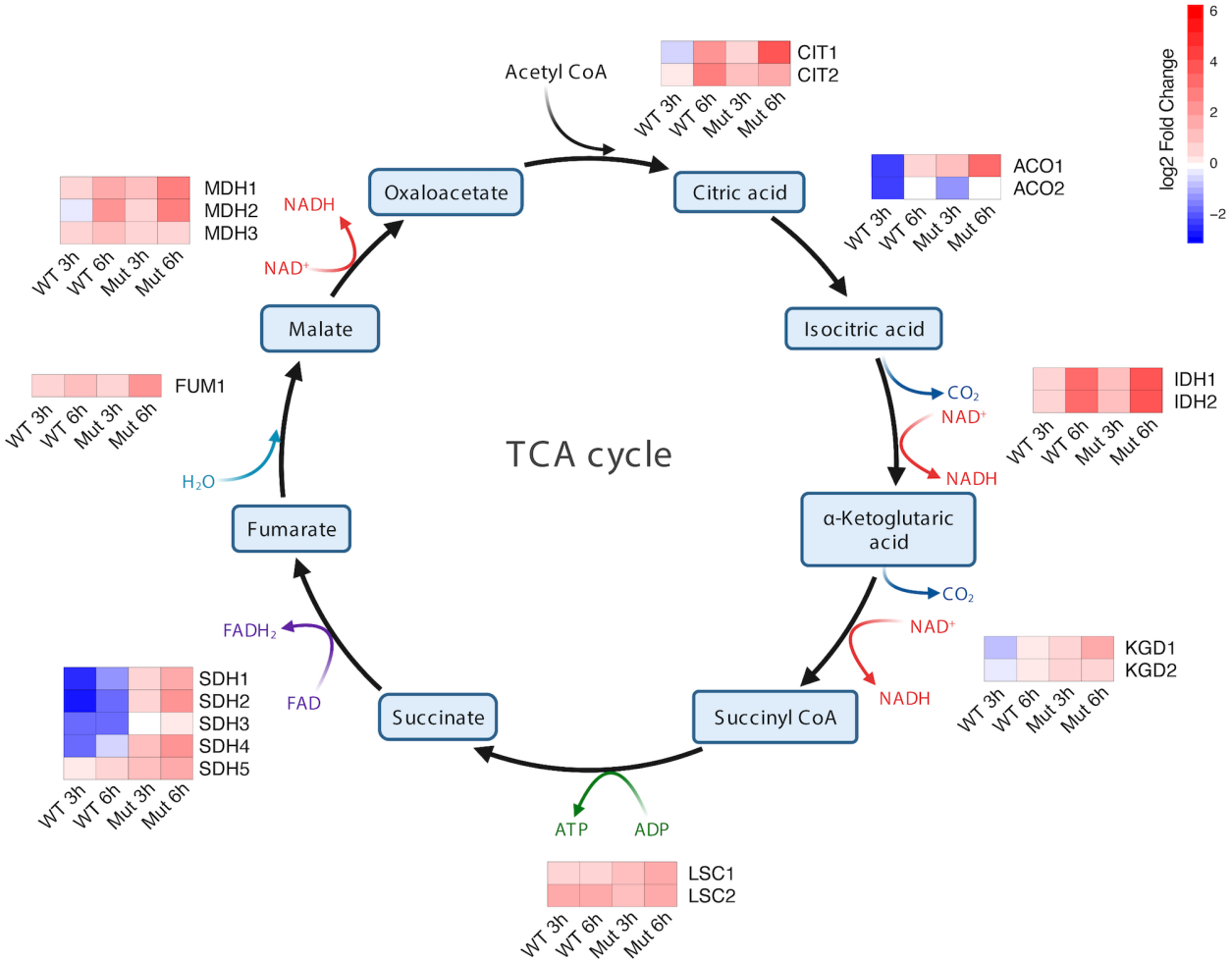

Fig S3. Heatmaps show log2 fold change in protein translation (Ribo-Seq) of differentially regulated genes of the TCA cycle during short-term (3h) and prolonged (6h) Fe deficiency in wild-type (WT) cells and the *cth1Δcth2Δ* mutant (Mut) (FDR<0.05).

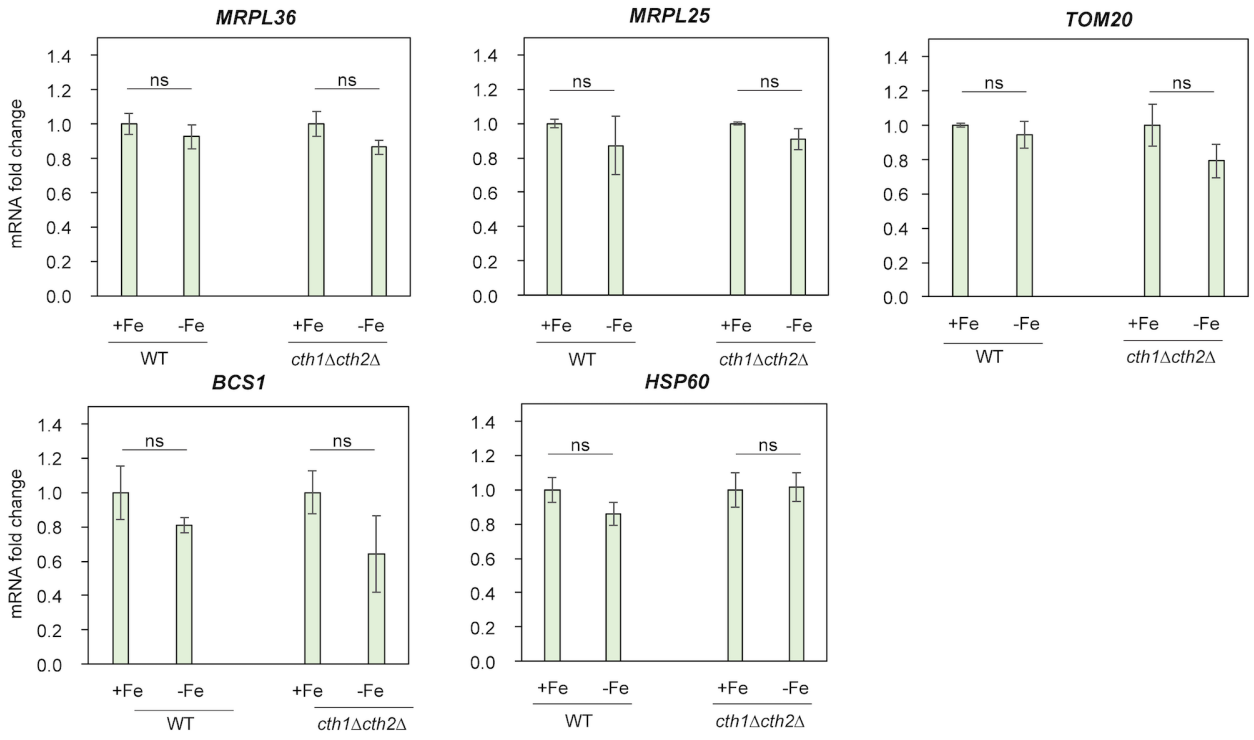

Fig S4. Fe deficiency does not affect transcription levels of mitochondrial ribosomal proteins. The expression of *MRPL36, MRPL25, TOM20, BCS1,* and *HSP60* was determined by RT-qPCR. Error bars represent SEM of three independent experiments; ns, non-significant (one-way ANOVA).

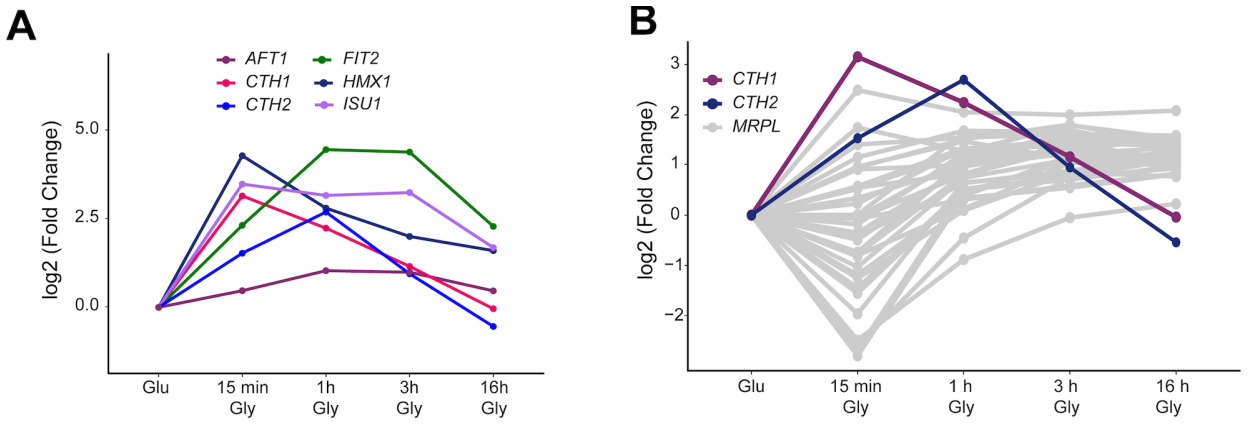

Fig S5. Expression of the Fe regulon genes (A) and mitochondrial ribosomal proteins of the large subunit (B) during the shift from the fermentable to non-fermentable carbon source. Cells were grown in YPD (Glu) medium to log phase and shifted to YPG (Gly) medium for the indicated time. Fold change in protein translation was measured by Ribo-Seq.

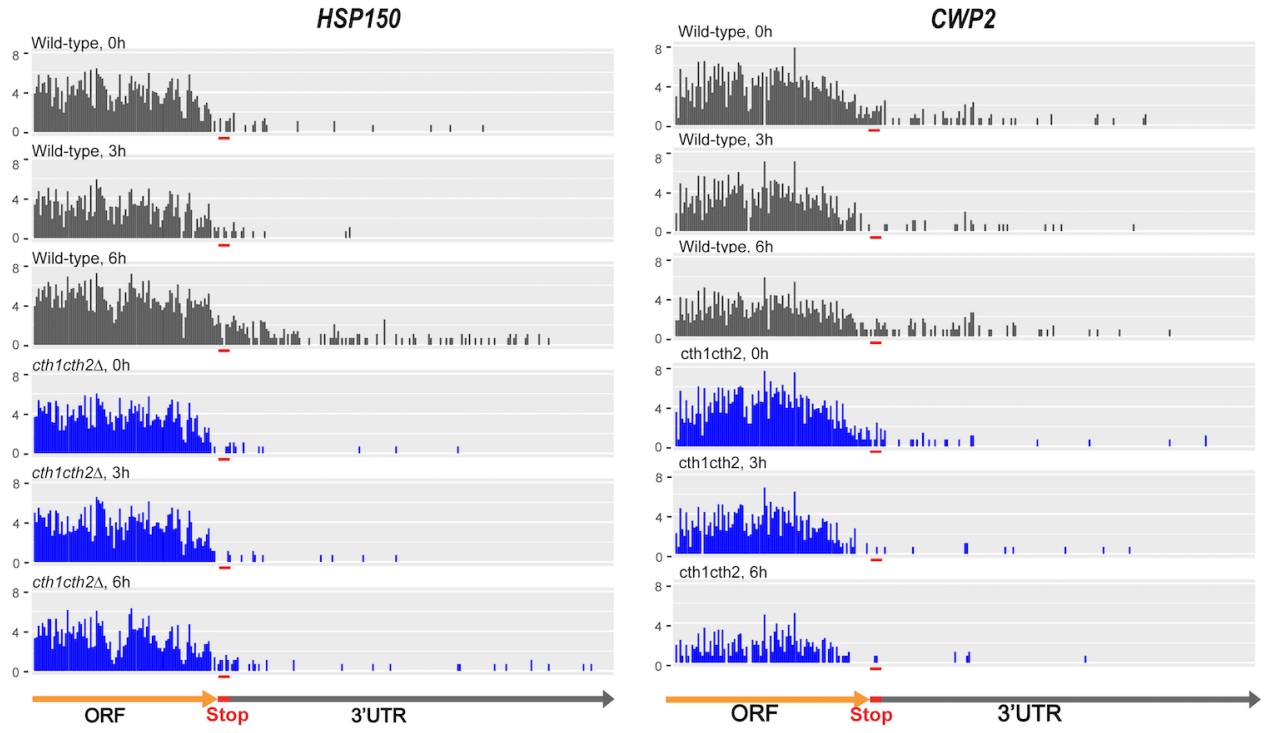

Fig S6. Fe deficiency leads to increased ribosome occupancy in the 3'UTRs. Ribosome occupancy at the 3'UTR of *HSP150* and *CWP2* mRNA during short (3h) and prolonged (6h) Fe deficiency (-Fe).

Table S1. Strains used in this study.

Strain	Genotype	Source
W303a	HTLU-2832-1B: *HIS3, TRP1, LEU2, URA3, ADE2, can1*	(Romero et al., 2019)
cth1Δcth2Δ	*W303a cthΔ2::KanMX, cthΔ1::hphB*	(Romero et al., 2019)
SED1-3'UTR-3xHA	*MATa his3Δ1 leu2Δ0 met15Δ0 ura3Δ0 SED1-3'UTR-3xHA-HIS3MX6*	(Young et al., 2015)
CWP2-3'UTR-3xHA	*MATa his3Δ1 leu2Δ0 met15Δ0 ura3Δ0 CWP2-3'UTR-3xHA-HIS3MX6*	(Young et al., 2015)
PUF3-HA-3'UTR	*MATa his3Δ1 leu2Δ0 met15Δ0 ura3Δ0 PUF3-HA-loxp-KanMX-loxp*	This study
PUF3-HA-3'UTR cth1Δcth2Δ	*MATa his3Δ1 leu2Δ0 met15Δ0 ura3Δ0 PUF3-HA-loxp-KanMX-loxp cthΔ2::hphB cthΔ1::NatMX*	This study